

A chiral rhenium complex with predicted high parity violation effects: synthesis, stereochemical characterization by VCD spectroscopy and quantum chemical calculations

Nidal Saleh,^a Samia Zrig,^{a,b} Thierry Roisnel,^a Laure Guy,^c Radovan Bast,^d Trond Saue,^d Benoît Darquié,^e and Jeanne Crassous^{*a}

With their rich electronic, vibrational, rotational and hyperfine structure, molecular systems have the potential to play a decisive role in precision tests of fundamental physics. For example, electroweak nuclear interactions should cause small energy differences between the two enantiomers of chiral molecules, a signature of parity symmetry breaking. Enantioenriched oxorhenium(VII) complexes *S*-(-)- and *R*-(+)-**3** bearing a chiral 2-methyl-1-thio-propanol ligand have been prepared as potential candidates for probing molecular parity violation effects via high resolution laser spectroscopy of the Re=O stretching. Although the rhenium atom is not a stereogenic centre in itself, experimental vibrational circular dichroism (VCD) spectra revealed a surrounding chiral environment, evidenced by the Re=O bond stretching mode signal. The calculated VCD spectrum of the *R* enantiomer confirmed the position of the sulfur atom *cis* to the methyl, as observed in the solid-state X-ray crystallographic structure, and showed the presence of two conformers of comparable stability. Relativistic quantum chemistry calculations indicate that the vibrational shift between enantiomers due to parity violation is above the target sensitivity of an ultra-high resolution infrared spectroscopy experiment under active preparation.

1 Introduction

Chirality is a challenge in diverse domains of chemistry, such as in the development and synthesis of molecules for pharmaceuticals,¹ agrochemicals, flavors, in nanotechnology^{2,3} or in asymmetric catalysis.⁴ Furthermore, studying unconventional chiral systems may be of great help for understanding the origin of prebiotic homochirality.⁵ More recently, very simple chiral molecules have been the object of interest for parity violation (PV) measurements, aiming at probing a tiny energy difference between the right- and left-handed enantiomers of a chiral molecule.^{6–8} During the last decade, we have been interested in observing this effect using an ultra-high resolution infra-red (IR) spectroscopy technique on a supersonic molecular beam.^{9–13} This collaboration between theoretical chemists, synthetic chemists, and spectroscopists, aiming at observing a vibrational PV frequency shift between enantiomers of chiral molecules, has recently been reviewed.¹²

A number of chiral compounds with heavy metals as the chiral centers have been theoretically studied for parity violation.^{14–19} In this context “chiral at metal” oxorhenium complexes have proven particularly suitable heavy transition metal complexes because they may fulfill all the requirements needed for a successful PV experiment. Indeed, the best candidate for our experimental test should i) show a large PV vibrational frequency difference of an intense fundamental band preferably within the CO₂ laser operating range (900–1100 cm⁻¹), ii) be available in large enantiomeric excess or, ideally, in enantiopure form and at the gram-scale, iii) have a reasonably simple structure so as to facilitate the spectroscopy and maintain a favourable partition function, and iv) allow the production of the supersonic expansion, thus sublime without decomposition.¹² Only a few simple “chiral at metal” rhenium complexes are known in the literature.^{20–29} Two classes of chiral complexes have been studied for PV experiments (see Figure 1): i) oxorhenium complexes such as **1**, bearing hydrotris(1-pyrazolyl)borate (Tp) ligand and a chiral bidentate ligand,²³ and ii) enantiopure “3+1” oxorhenium complexes bearing a tridentate sulfated ligand and a monodentate halogen (such as **2**) or a chalcogenated ligand.^{24,25} Methyltrioxorhenium (MTO) is an efficient catalyst for reactions such as for instance epoxidation of olefins.³⁰ More interestingly for our purposes, it sublimes very easily¹³ (vapour pressure of a few tenths of mbars at room temperature). Furthermore, a few examples of sublimable MTO derivatives have been described in the literature²⁹ and the strategy of preparing simple chiral easily sublimable MTO derivatives seems an appealing route

^a Institut des Sciences Chimiques de Rennes, UMR 6226 CNRS - Université de Rennes 1, Campus de Beaulieu, F-35042 Rennes Cedex, France. Fax: (+33) 2-23-23-69-39; Tel: (+33) 2-23-23-57-09; E-mail: jeanne.crassous@univ-rennes1.fr

^b Present address: ITODYS, UMR 7086 CNRS, Université Paris Diderot, Sorbonne Paris Cité, F-75205 Paris Cedex 13, France

^c Laboratoire de Chimie, UMR 5182 Ecole Normale Supérieure de Lyon-CNRS, F-69364 Lyon 07, France

^d Laboratoire de Chimie et Physique Quantiques, UMR 5626, CNRS et Université de Toulouse 3 (Paul Sabatier), 118 route de Narbonne, F-31062 Toulouse, France

^e Laboratoire de Physique des Lasers, Université Paris 13, Sorbonne Paris Cité, CNRS, F-93430, Villetaneuse, France

to find a suitable candidate molecule for the experimental PV test. Our target molecule was therefore the enantiopure oxorhenium complex **3** which is a chiral derivative of MTO bearing a 2-methyl-thiopropionate ligand. In this article we detail the synthesis, the stereochemical characterization and vibrational circular dichroism (VCD) spectroscopy of complex **3** to examine the dissymmetric environment around the rhenium atom. We furthermore carry out relativistic quantum chemical calculations of the vibrational frequency shift associated with the parity violation energy difference between enantiomers of complex **3**. Experimental and computational details are given in sections 7 and 8, respectively.

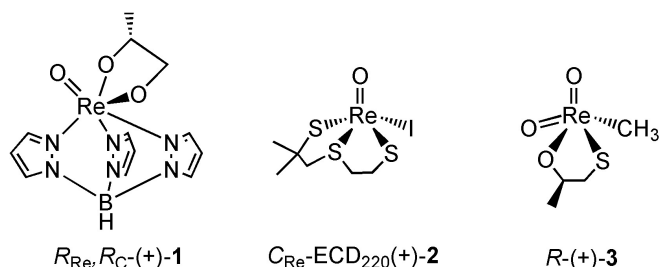


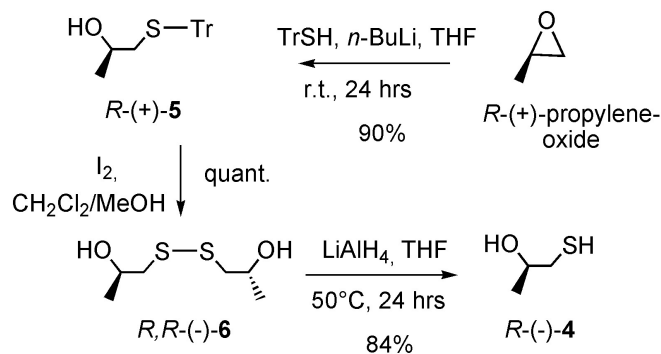
Fig. 1 Examples of chiral oxorhenium complexes studied for parity violation effects (refs. 23–25 and this work).

2 Synthesis

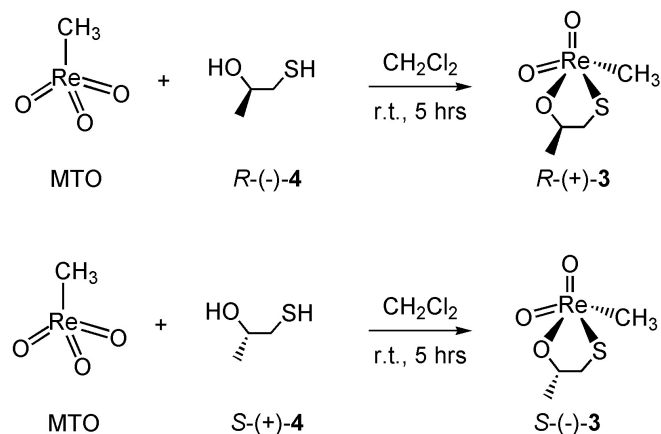
The synthesis of the enantiomers of the 2-methyl-thiopropanol ($R(-)$ - and $S(+)$ -**4**) ligands was achieved using enantiomerically pure propylene oxide as the starting precursor as described in Scheme 1. The regioselective opening of $R(+)$ - and $S(-)$ -propylene oxide with trityl thiol³¹ gave respectively the alcohols $R(+)$ - and $S(-)$ -**5** with 90% yield. The subsequent deprotection followed by *in situ* oxidation with iodine yielded quantitatively disulfide $R,R(-)$ - and $S,S(+)$ -**6**, which were finally reduced by $LiAlH_4$ to $R(-)$ - and $S(+)$ -**4** with 84% yield. Their optical rotation and all spectroscopic characteristics are in agreement with already published results.³² The $(+)$ - and $(-)$ -**3** enantiomeric complexes were then prepared by reacting the enantiopure $R(+)$ - and $S(-)$ -**4** with MTO in dry dichloromethane according to a previously reported procedure³³ as depicted in Scheme 2.

3 X-ray crystallography

Single crystals of a racemic sample of the oxorhenium(VII) complex **3** were obtained after sublimation under vacuum. Due to significant disorder of the methyl group coming from the two possible configurations of the stereogenic carbon center, the X-ray structure of complex **3** was solved in the non-centrosymmetric P21 space-group. A final Flack parameter of



Scheme 1. Synthesis of the enantioenriched ligand 2-methyl-1-thiopropanol $R(-)$ -**4** from $R(+)$ -propylene oxide.



Scheme 2 Synthesis of the enantioenriched oxorhenium complexes $R(+)$ - and $S(-)$ -**3** from MTO and enantioenriched 2-methyl-1-thiopropanol $R(-)$ - and $S(+)$ -**4**.

0.46 was obtained, indicating the presence of a racemic mixture. As depicted in Figure 2, the rhenium center is penta-coordinated, the C1 atom is *trans* to the O3 oxygen, and the $Re, O3, S, C1$ lie in the same plane, while the two oxo groups are symmetrically placed on each side of this plane (for example, angles $O3-Re-O1$: 100.66° and $O3-Re-O2$: 105.03° for one of the four independent molecules of the unit cell). Consequently the oxygen atoms O1 and O2 only differ in their chemical environment due to the proximity of the asymmetric carbon C2. The $Re-O$ bond lengths in the two oxo groups are classic (1.675 \AA to 1.687 \AA). Since oxorhenium complexes most often crystallize in a square pyramidal geometry, with an oxygen atom of the $Re=O$ bond being placed in the apical position, the geometry around the rhenium atom is rather uncommon.³⁴ Finally, in the solid state the methyl group C3 is placed in the equatorial position, and the dihedral angle $O3-C2-C4-S$ within the five-membered ring is about -51° . The conformational space of complex **3** has been further explored

by density functional theory (DFT) calculations, as discussed in the next section.

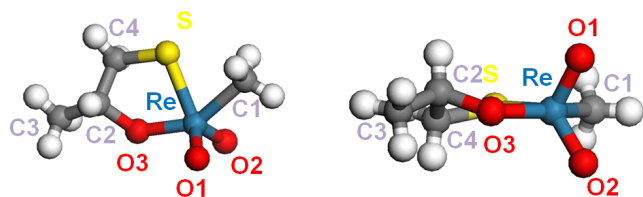


Fig. 2 X-ray crystallographic structure of the complex *R*-(+)-**3**.

4 VCD spectroscopy

For our fundamental physics purposes we would like simple chiral molecules containing one or more heavy metals, preferably as a stereogenic center or at least in its vicinity. The former is nonetheless not straightforwardly realized.^{24,25} From the experimental viewpoint, VCD spectroscopy, which has been under-explored in chiral complexes, can be a very powerful tool to study the dissymmetric environment around the metal center.^{35–38} In order to get more insight into the latter, the IR and VCD spectra of complex **3** were calculated and compared to experiment.

Our first computational goal, however, was to find a set of stable conformers of complex **3** for a subsequent calculation of IR and VCD spectra. Using the *R* enantiomer and starting from the X-ray structure in which the S–Re bond is placed in *cis* position to the Re–Me one, we carried out a potential energy scan along the O3–C2–C4–S dihedral angle at the DFT level using the B3LYP functional (def2-TZVPP basis³⁹). We identified two stable conformers, **3a-c1** and **3a-c2** at the O3–C2–C4–S dihedral angles -39.8° and $+37.5^\circ$, respectively. As shown in Figure 3, the conformers are separated by a barrier of almost 10 kJ/mol and differ in energy by 3.4 kJ/mol, the latter corresponding to Boltzmann populations of 80%:20% at 296 K.

The conformers **3a-c1** and **3a-c2** are not the only possible realizations of the ligation and we have extended the study by optimizing the structures of corresponding **3b-c1** and **3b-c2** conformers where the O–CHMe–CH₂–S ligand is connected to Re with S–Re *trans* to Re–Me. The conformers **3b-c1** and **3b-c2** are separated by 5.4 kJ/mol, corresponding to Boltzmann populations of 90%:10% at 296 K. Conformer **3b-c1** is, however, 18.4 kJ/mol higher in energy compared to **3a-c1**, and we will in the following be able to confirm the predominance of form **3a-c1** from simulation of the spectra. Before turning to the discussion of simulated spectra we would first like to discuss the energetic separation between the four studied conformers. To clarify whether the energetic preference for **3a-c1** was sterically controlled by the Me group at the C2 atom or

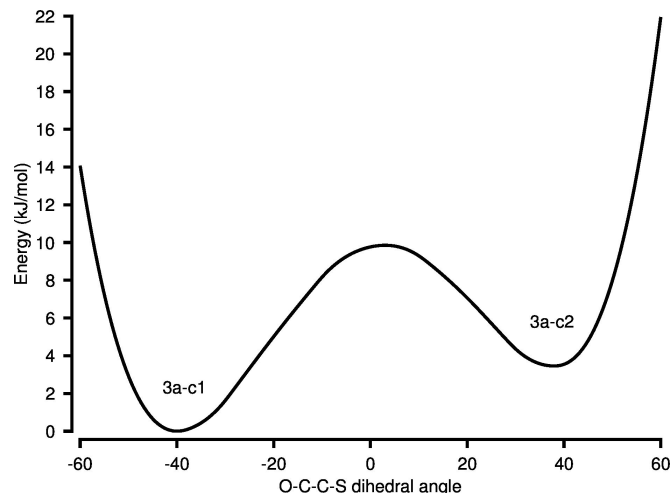


Fig. 3 Potential energy scan of complex **3** along the O3–C2–C4–S dihedral angle (B3LYP, def2-TZVPP basis, all other coordinates relaxed).

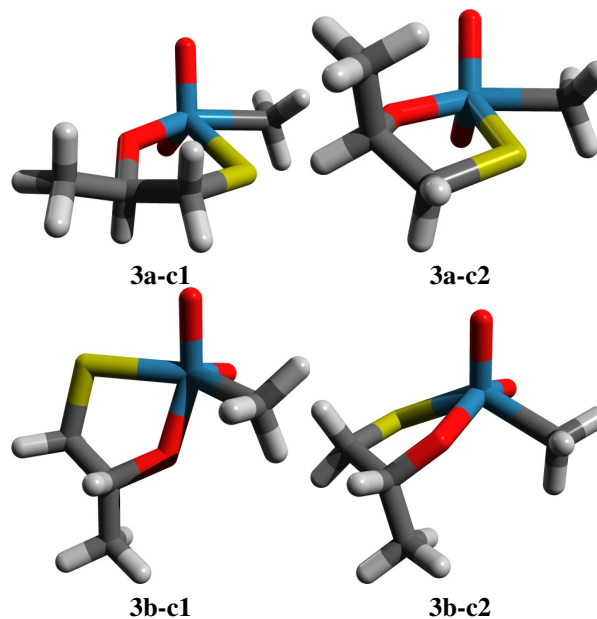


Fig. 4 B3LYP (def2-TZVPP basis) equilibrium structures of the theoretically studied conformers.

electronically controlled according to the HSAB principle⁴⁰ we have optimized structures for **3a'-c1**, **3a'-c2**, **3b'-c1**, and **3b'-c2** conformers, where the Me group at the C2 atom has been replaced by a H atom. By doing this we find that the conformations **c1** and **c2** are energetically almost equal for both **3a'** and **3b'** (separated by less than 0.02 kJ/mol, but retaining the barrier heights) while the difference between **3a'-c1** and **3b'-c1** remains 18.0 kJ/mol, as compared to the difference of 18.4 kJ/mol between **3a-c1** and **3b-c1**. This indicates that the energy difference between **c1** and **c2** is sterically controlled by the Me group attached to the C2 atom and can be tuned by bulkier ligands, while the preference for **3a** over **3b** is electronically controlled by the O (HSAB harder) and S (HSAB softer) atoms.⁴⁰ This theoretical study nicely illustrates the concept of the *trans*-effect in coordination chemistry.

In order to verify the findings obtained using the relative energies and to obtain more insight into the chiral environment around the metal center, we next compared simulated IR and VCD spectra of complexes **3a** and **3b** to the experimentally recorded spectra. The experimentally recorded IR spectrum of complex **3a** in CD₂Cl₂ is shown as a dashed line in Figure 5. The IR signature is identical for both enantiomers (at this resolution). The experimental VCD spectra of *R*-(+)-**3** and *S*-(-)-**3** enantiomers in CD₂Cl₂ are shown in Figure 6 in red and blue color, respectively. The experimental VCD spectra show a mirror-image relationship and exhibit a strong absorption band at 1012 cm⁻¹ (dissymmetry factor $\Delta\epsilon/\epsilon = 1.5 \times 10^{-4}$) which corresponds to the oxorhenium symmetric bond stretching (the antisymmetric stretch, although not accessible to our VCD spectrometer, is also visible on the experimental IR spectrum of Figure 5 at ~ 980 cm⁻¹). The presence of such a band indicates a chiral environment around the rhenium atom, although the rhenium is not a stereogenic center in itself.

Comparing the observed IR and VCD spectra with the calculated spectra for the Boltzmann-averaged **3a** and **3b** we note that the match for conformer **3a** is not perfect, but it is better than for **3b**, which we expect based on energetic arguments. We should also note that the agreement between experimental and simulated spectra seems to be better for the Stuttgart ECP/6-31Gd basis, already employed in Refs. 23 and 24, than for the def2-TZVPP basis, although the latter is a more flexible basis which we consider close to basis set limit at the DFT level. This can probably be attributed to error cancellation effects. Overall, the VCD spectrum calculated for the *R*-stereochemistry using the Stuttgart ECP/6-31Gd basis set reproduces the experimental spectrum for the (+) enantiomer well, except for the peak at 1160 cm⁻¹. The discrepancy may be due to the flexibility of the five-membered rhenacycle in solution that induces additional conformations. In conclusion this conformational analysis and IR/VCD studies show that although the Re atom is not strictly speaking a stereogenic center, the Re–O stretching bond at 1012 cm⁻¹ has a strong well-defined

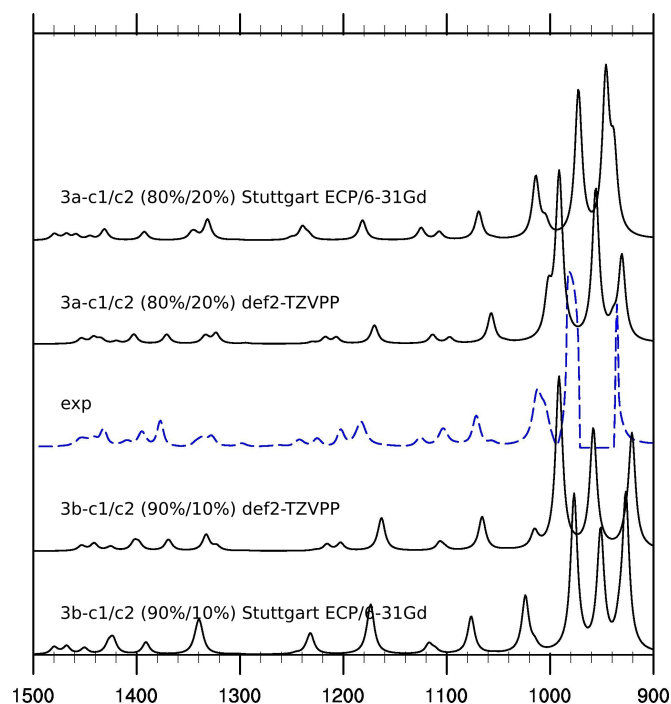


Fig. 5 Overlay of the simulated Boltzmann-averaged IR spectra for complex **3** (black solid lines, B3LYP, scaled), and the experimental spectrum (blue dashed line, 90 mg in 1 mL of CD₂Cl₂, 100 μ m cell, 4 cm⁻¹ resolution, 3000 scans).

chiroptical signature that is a testimony of the chiral environment around the metal center. In our opinion this makes the enantiopure chiral oxorhenium(VII) complex **3** a good candidate for a PV measurement. For this reason, the PV vibrational shifts associated with the Re–O stretching modes were predicted by relativistic DFT calculations, as described in the following.

5 Calculated PV shifts

Table 1 summarizes the results of our computational study of the selected two conformers **3a-c1** and **3a-c2** (see Figure 4), where we have studied the symmetric and anti-symmetric Re=O stretching mode frequencies using HF and two density functional approximations, the hybrid B3LYP and the non-hybrid PBE exchange-correlation functionals. Comparing the 4-component DC Hamiltonian PV fundamental transition frequency differences $\Delta\nu_{0\rightarrow1}$ (Table 1), we can first note that our calculations predict PV vibrational frequency differences in the sub-Hz range, above the anticipated experimental uncertainty in the frequency difference measurement.¹² This is an encouraging result for our collaboration. However, from the

Table 1 Calculated reduced masses (in amu), vibrational transition frequencies (in cm^{-1}) of the anti-symmetric and symmetric Re=O stretches for the conformers **3a-c1** and **3a-c2**, with corresponding 4-component DC Hamiltonian PV fundamental transition frequency differences $\Delta\nu_{0\rightarrow 1}$ (in Hz).

| Conformer | Mode | Method | Red. mass | Harmonic | Fundamental | PV shift |
|--------------|------|--------|-----------|----------|-------------|----------|
| 3a-c1 | asym | HF | 14.2074 | 1106 | 1102 | -0.211 |
| | | B3LYP | 15.7268 | 986 | 982 | 0.078 |
| | | PBE | 15.8522 | 951 | 944 | 0.195 |
| | sym | HF | 8.7326 | 1174 | 1165 | 0.344 |
| | | B3LYP | 12.8095 | 1022 | 1010 | 0.150 |
| | | PBE | 14.8015 | 980 | 968 | 0.036 |
| 3a-c2 | asym | HF | 15.2424 | 1106 | 1102 | 0.219 |
| | | B3LYP | 15.7515 | 985 | 981 | -0.119 |
| | | PBE | 15.8566 | 950 | 944 | -0.271 |
| | sym | HF | 8.4859 | 1175 | 1165 | -0.056 |
| | | B3LYP | 7.2491 | 1021 | 1010 | -0.170 |
| | | PBE | 13.1114 | 979 | 966 | -0.084 |

theoretical point of view, the significant variation of the calculated PV transition frequency differences is troubling, showing high sensitivity to both the method applied (HF or density functional approximations) and to structural changes. Comparing HF with B3LYP and PBE we see that the order of magnitude can change as well as the sign. In principle we should rather trust the DFT calculations, since they incorporate electron correlation, but the performance of DFT functionals with respect to PV shifts for these heavy element compounds needs further study (in progress in our laboratory). If we single out one method then a slight modification of the structural periphery seems to have a major effect on the chiral environment around the heavy atom (as exemplified by the sign change between the PV shifts for **3a-c1** and **3a-c2** in Table 1). This makes parity violation *chemically* interesting, as detailed analysis of the underlying mechanism may provide a deeper understanding of the electronic structure of chiral molecules. It should be emphasized that conformational averaging, as carried out in the simulation of IR and VCD spectra in section 4, is not an issue in the ultra-high resolution experiment since it will resolve individual lines of each conformer.

6 Conclusion

We have reported the synthesis and resolution, characterization, and computational study of a new oxorhenium(VII) chi-

ral compound. It is designed for the molecular beam experiment, proposed in Ref. 12, dedicated to the observation of PV effects via high-resolution vibrational spectroscopy. As an MTO derivative, this solid-state complex is expected to sublime easily, a key aspect to allow gas phase studies. Measurements and calculations show that the normal mode associated with the Re=O stretch lies within the CO₂ laser operating range. Enantioselective synthesis was developed for the preparation of enantioenriched complexes. DFT calculations allowed the identification of four conformers (**3a-c1**, **3a-c2**, **3b-c1** and **3b-c2**, see Figure 4) as well as the rationalization of their relative stability. We find that the stability **3a** with respect to **3b** can be attributed to a *trans* effect, whereas the smaller energy difference of **c1** with respect to **c2** arises from a steric effect. The experimental VCD spectra are accordingly dominated by the two most stable conformers **3a-c1** and **3a-c2**, as verified by their theoretical simulation which furthermore allowed determination of their absolute configuration.

The VCD study has brought to light the chiral environment surrounding the rhenium atom, albeit not a stereogenic centre in itself. Motivated by this observation, the vibrational transition frequency differences between the enantiomers due to PV was calculated using Hartree-Fock (HF) and DFT. These results confirm the 0.1 Hz order of magnitude for DFT PV vibrational frequency differences, as reported earlier for oxorhenium complexes, which would be above the 0.01 Hz experi-

mental uncertainty expected in the frequency difference measurement.¹² The present study puts emphasis on the sensitivity of the PV vibrational frequency difference to the chemical environment around the rhenium centre, as reported earlier by us.²⁵ This work represents an important step towards the first experimental observation of PV in molecular systems.

7 Experimental details

7.1 General

Most experiments were performed using standard Schlenk techniques. Solvents were freshly distilled under argon from sodium/benzophenone (THF) or from phosphorus pentoxide (CH_2Cl_2). Starting materials were purchased from ACBR (MTO) or from Aldrich. The synthesis of ligand **4** enantiomers was performed by using a modified procedure.³² Column chromatography purifications were performed in air over silica gel (Merck Geduran 60, 0.063–0.200 mm). ^1H and ^{13}C NMR spectra were recorded on a Bruker AM300. ^{13}C NMR spectra at 50.4 MHz were recorded on a Bruker DPX 200. Chemical shifts were reported in parts per million (ppm) relative to $\text{Si}(\text{CH}_3)_4$ as external standard and compared to the literature. IR and VCD spectra were recorded on a Jasco FSV-6000 spectrometer. Specific rotations (in $\text{deg cm}^2\text{g}^{-1}$) were measured in a 10 cm thermostated quartz cell on a Jasco P1010 polarimeter. Elemental analyses were performed by the group CRMPO, University of Rennes 1. CCDC reference number 910638 contains the crystallographic data for complex **3**. These data can be obtained free of charge at www.ccdc.cam.ac.uk/conts/retrieving.html or from the Cambridge Crystallographic Data Center, 12 union Road, Cambridge CB2 1EZ, UK; Fax: (internat.) +44-1223-336-033; E-mail: deposit@ccdc.cam.ac.uk.

***S*-(−)-1-(tritylthio)propan-2-ol (*S*-(−)-**5**).** *n*-BuLi (4.78 mmol, 2.5 M, 1.91 mL) was added dropwise to a triphenylmethanethiol solution (4.67 mmol, 1.29 g) in 15 mL distilled THF cooled at 0°C, where a red-rose color persisted. *S*-(−)-propylene oxide (4.28 mmol, 0.3 mL) was then added dropwise at 0°C with a change in color to pale yellow. The reaction mixture was stirred over night, quenched with 20% AcOH in 20 mL methanol, diluted with water, and then extracted with ethyl acetate. Purification over silica gel column chromatography (pentane/ethyl acetate, 9:1) provided *S*-(−)-**5** with 90% yield. ^1H NMR (300 MHz, CDCl_3) δ 7.40–7.50 (6 H, m), 7.19–7.37 (9 H, m), 3.43 (1 H, sxt, $J = 6.2$ Hz), 2.40 (1 H, d, $J = 1.1$ Hz), 2.38 (1 H, s), 1.07 (3 H, d, $J = 6.1$ Hz). $[\alpha]_D^{23} = -54.4$ ($C = 10^{-3}$ M, CH_2Cl_2) ref. 32: $[\alpha]_D^{23} = -27.5$ ($C = 3.35 \times 10^{-3}$ M, CHCl_3). The same procedure was used for the preparation of the *R*-(+)-**5** enantiomer $[\alpha]_D^{23} = +54.4$ ($C = 10^{-3}$ M, CH_2Cl_2).

***S,S*-(+)-1,1'-disulfanediybis(propan-2-ol) ((*S,S*)-(+)-**6**).**

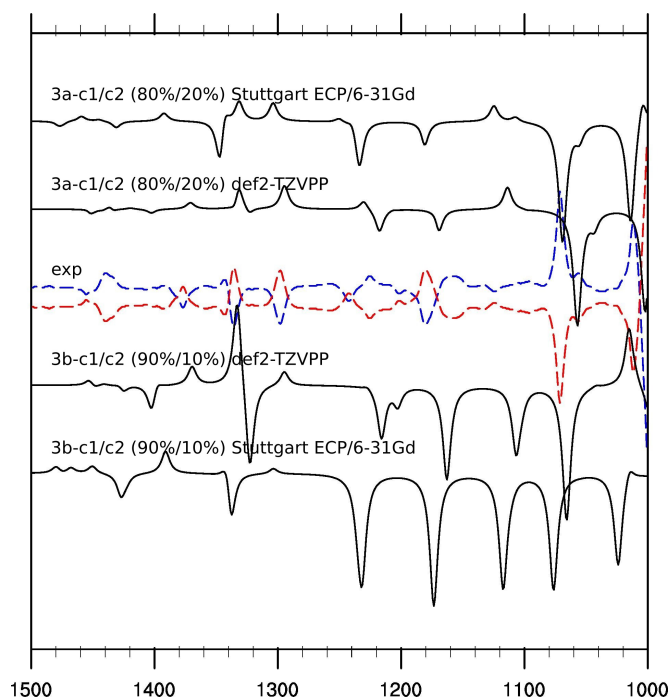


Fig. 6 Overlay of the simulated Boltzmann-averaged VCD spectra for complex *R*-**3** (black solid lines, B3LYP, scaled), and the experimental spectra (red and blue dashed lines correspond respectively to (+)-**3** and (−)-**3**, 90 mg in 1 mL of CD_2Cl_2 , 100 μm cell, 4 cm^{-1} resolution, 3000 scans).

S-1-(tritylthio)propan-2-ol (*S*-(-)-**5**) (300 mg, 0.897 mmol) dissolved in 50 mL DCM/Methanol (9:1) solution was added in portions (30 min) over Iodine solution, 1.1 g in 500 mL DCM/Methanol (9:1). The reaction mixture was stirred at room temperature for 30 min, quenched with 10% aqueous Sodium thiosulfate and washed with brine. The organic layer was separated and the aqueous layer was extracted with ethyl acetate twice, dried over MgSO₄, and concentrated in vacuum to provide a dark brown precipitate which was purified by silica gel chromatography (5% ethanol/chloroform) to provide (2*S*,2'*S*)-(+)-**6** as a yellow-brown oil (99%). ¹H NMR (300 MHz, CDCl₃) δ 3.93–4.25 (1 H, m), 2.90 (1 H, dd, *J* = 13.6, 3.4 Hz), 2.69 (1 H, dd, *J* = 13.7, 8.5 Hz), 2.41 (1 H, br. s.), 1.31 (3 H, d, *J* = 6.0 Hz). ¹³C NMR (75 MHz, CDCl₃) δ 65.9, 47.5, 22.0. [α]_D²³ = +232 (*C* = 2.7 × 10⁻³ M, CH₂Cl₂), ref. 32: [α]_D²³ = +199.3 (*C* = 1.96 × 10⁻³ M, CHCl₃). The same procedure was used for the preparation of the ((*R*,*R*)-(-)-**6**) enantiomer [α]_D²³ = -236 (*C* = 2.7 × 10⁻³ M, CH₂Cl₂).

***S*-(+)-2-methyl-thiopropanol (*S*-(+)-**4**).** 100 mg of (*S*,*S*)-1,1'-disulfanediylbis(propan-2-ol) ((*S*,*S*)-**6**) in THF was added dropwise to a stirring solution of LAH (3 eq.) in THF at 0°C, then stirred for 24 hrs at 50°C. The reaction was quenched with AcOH and then extracted with ether, dried over MgSO₄, and concentrated under vacuum to obtain *S*-(+)-**4** (42.2 mg, 84%) as a colorless oil. ¹H NMR (300 MHz, CDCl₃) δ 3.77–3.86 (m, 1 H), 2.74 (dd, 1 H, *J* = 14.1, 3.6 Hz), 2.5 (dd, 1 H, *J* = 13.4 Hz, 7.4 Hz), 1.27 (d, 3 H, *J* = 6.0 Hz). [α]_D²³ = +172 (*C* = 5.10 × 10⁻² M, CH₂Cl₂). The same procedure was used for the preparation of the *R*-(-)-**4** enantiomer. [α]_D²³ = -166 (*C* = 5.10 × 10⁻² M, CH₂Cl₂). ¹³C NMR (75 MHz, CDCl₃) δ 68.3, 32.8, 21.6.³²

***S*-(-)-**3** complex.** Methyltrioxorhenium (110 mg, 0.44 mmol) was dissolved in 10 mL distilled DCM, *S*-(+)-2-methyl-thiopropanol (0.44 mmol, 40.1 mg) was then added, and the reaction mixture was stirred overnight under argon. Solvent was removed under reduced pressure to obtain *S*-(-)-**3** as a yellow-orange precipitate. ¹H NMR (300 MHz, CDCl₃) δ 5.30 (1 H, sxt, *J* = 6.1 Hz), 3.84 (1 H, dd, *J* = 11.3, 5.3 Hz), 3.46 (1 H, dd, *J* = 11.7, 7.2 Hz), 2.50 (3 H, s), 1.51 (3 H, d, *J* = 6.1 Hz). ¹³C NMR (75 MHz, CDCl₃) δ 90.6, 46.2, 29.7, 20.8. [α]_D²³ = -17 (*C* = 3.1 × 10⁻³ M, CH₂Cl₂). The same procedure was used for the preparation of the *R*-(+)-**3** enantiomer and for racemic **3**. [α]_D²³ = +17 (*C* = 3.1 × 10⁻³ M, CH₂Cl₂).

7.2 VCD measurements

Samples of (+)-**3** and (-)-**3**, ≈ 9 mg/100 μL CD₂Cl₂, were placed in a 100-μm path length cell with BaF₂ windows. IR and VCD spectra were recorded on a Jasco FVS-6000 VCD spectrometer with 3000 scans acquired and averaged at 4 cm⁻¹ resolution. An overlay of the observed spectra for the two enantiomers, combined with the simulated Boltzmann-

averaged VCD spectrum for complex *R*-**3** in two different basis sets, is presented in Figure 6. The average VCD spectrum of the two enantiomers was used as the VCD baseline.

8 Computational details

The optimized molecular structures and the corresponding IR and VCD spectra were obtained using the Gaussian 09 package⁴¹ employing the default harmonic approximation⁴² and using Kohn–Sham DFT together with the hybrid functional B3LYP^{43,44} (employing the VWN3⁴⁵ correlation functional). In addition we have also employed HF and the PBE⁴⁶ functional to obtain the optimized structures and the harmonic force field for the subsequent *E*_{PV} calculations. We have used two different basis sets: Ahlrichs' def2-TZVPP^{39,47} (all atoms) to obtain a result close to the basis set limit, and the less flexible 6-31Gd⁴⁸ (all atoms except Re) in combination with the Stuttgart/Dresden ECP-60-MWB⁴⁷ (Re) for compatibility with a previous VCD study of a similar compound.²⁴ The vibrational frequencies were scaled by 0.97 and the calculated intensities were converted to Lorentzian bands with 4 cm⁻¹ half-width at half-maximum for comparison to experiment.

In order to calculate the PV vibrational frequency shift we have performed single-point energy and PV energy calculations using the DIRAC12 program⁴⁹ following the normal mode coordinates taken from the corresponding Gaussian 09 calculation. The single-point energies, now based on the 4-component relativistic Dirac-Coulomb (DC) Hamiltonian, calculated along the effective core potential normal mode provided the anharmonic potential for the numerical solution of the vibrational wave functions by the Numerov–Cooley algorithm.^{50,51}

The PV vibrational frequency shift $\nu_{m \rightarrow n}$ for the $m \rightarrow n$ vibrational transition (in our case 0 → 1) is obtained using

$$h\Delta\nu_{m \rightarrow n} = 2(\langle n | E_{PV}(q_R) | n \rangle - \langle m | E_{PV}(q_R) | m \rangle), \quad (1)$$

where $|n\rangle$ and $|m\rangle$ are the corresponding Numerov–Cooley vibrational wave functions. $E_{PV}(q_R)$ is the PV energy along the normal mode coordinate q of the *R* enantiomer, evaluated as an expectation value of the operator

$$\hat{H}_{PV} = \sum_K \hat{H}_{PV,K}; \quad \hat{H}_{PV,K} = \frac{G_F}{2\sqrt{2}} Q_{w,K} \sum_i \gamma^5 \rho_K(\mathbf{r}_{iK}), \quad (2)$$

in which appears the weak nuclear charge $Q_{w,K} = Z_K(1 - 4\sin^2\theta_W) - N_K$ with Z_K and N_K representing the number of protons and neutrons in nucleus *K*, respectively, and $\sin^2\theta_W = 0.2319$ is the employed Weinberg parameter. The normalized nuclear charge densities ρ_K , in this work represented by Gaussian distributions,⁵² restrict integration over electron coordinates \mathbf{r}_i to nuclear regions, thus providing a natural partitioning of the operator in atomic contributions $\hat{H}_{PV,K}$. Finally, γ^5

is one of the Dirac matrices, Eq. (3), with $1_{2 \times 2}$ and $0_{2 \times 2}$ being the 2×2 identity and null matrices, respectively

$$\gamma^5 = \begin{bmatrix} 0_{2 \times 2} & 1_{2 \times 2} \\ 1_{2 \times 2} & 0_{2 \times 2} \end{bmatrix}. \quad (3)$$

The Fermi coupling constant $G_F = 2.22254 \times 10^{-14} E_h a_0^3$ demonstrates the minuteness of the PV effect.

We have calculated PV energies at the HF level as well as using the density functionals B3LYP^{43,44} and PBE,⁴⁶ all in a 4-component relativistic framework. For the DC single-point calculations we have employed uncontracted cc-pVDZ basis sets⁵³ for all atoms except Re, for which we have used the basis sets employed in Ref. 25. The small component basis sets were generated by restricted kinetic balance imposed in the canonical orthonormalization step.⁵⁴ The two-electron Coulomb integrals (SS|SS), involving only the small components, were neglected in all calculations and the energy corrected by a simple point-charge model.⁵⁵

9 Acknowledgment

We thank the Ministère de l'Éducation Nationale, de la Recherche et de la Technologie, and the Centre National de la Recherche Scientifique (CNRS). This work is part of the project NCPCHEM 2010 BLAN 724 3 funded by the Agence Nationale de la Recherche (ANR, France). This work has received support from the high performance computing centre "Calcul en Midi-Pyrénées" (CALMIP) through a grant of computer time.

References

- 1 "Chirality in Drug Research", E. Francotte, W. Lindner (eds.), Wiley-VCH, 2006.
- 2 "Chirality at the Nanoscale: Nanoparticles, Surfaces, Materials and more", D. Amabilino (ed.), Wiley-VCH, 2009.
- 3 Special issue on chirality at the nanoscale: D. Amabilino (Guest Editor), *Chem. Soc. Rev.* 2009, **38**, 659.
- 4 "New Frontiers in Asymmetric Catalysis", K. Mikami, M. Lautens (eds.), Wiley-VCH, 2007.
- 5 C. Viedma, P. Cintas *Isr. J. Chem.*, 2011, **51**, 997 and references therein.
- 6 "On Chirality and the Universal Asymmetry: Reflections on Image and Mirror Image", G. H. Wagnière (ed.), Wiley-VCH, 2007.
- 7 M. Quack, *Angew. Chem. Int. Ed.*, 2002, **41**, 4618.
- 8 M. Avalos, R. Babiano, P. Cintas, J. L. Jimenez, J. C. Palacios, *Tetrahedron Asymmetry*, 2000, **11**, 2845.
- 9 J. Crassous, F. Monier, J.-P. Dutasta, M. Ziskind, C. Daussy, C. Grain and C. Chardonnet, *ChemPhysChem*, 2003, **4**, 541.
- 10 J. Crassous, C. Chardonnet, T. Saue and P. Schwerdtfeger, *Org. Biomol. Chem.*, 2005, **3**, 2218.
- 11 C. Chardonnet, C. Daussy, O. Lopez, A. Amy-Klein, In: Maroulis G, Simos T (eds.) "Trends and Perspectives in Modern Computational Science." Vol. 6, Lecture Series on Computer and Computational Sciences, 2006. 324–331.
- 12 B. Darquié, C. Stoeffler, A. Shelkovich, C. Daussy, A. Amy-Klein, C. Chardonnet, S. Zrig, L. Guy, J. Crassous, P. Soulard, P. Asselin, T. R. Huet, P. Schwerdtfeger, R. Bast, T. Saue, *Chirality*, 2010, **22**, 870.
- 13 C. Stoeffler, B. Darquié, A. Shelkovich, C. Daussy, A. Amy-Klein, C. Chardonnet, L. Guy, J. Crassous, T. R. Huet, P. Soulard, P. Asselin, *Phys. Chem. Chem. Phys.*, 2011, **13**, 854.
- 14 J. K. Lærdahl, P. Schwerdtfeger, H. M. Quiney, *Phys. Rev. Lett.*, 2000, **84**, 3811.
- 15 P. Schwerdtfeger and R. Bast, *J. Am. Chem. Soc.*, 2004, **126**, 1652.
- 16 P. Schwerdtfeger, J. Gierlich, T. Bollwein, *Angew. Chem. Int. Ed.*, 2003, **42**, 1293.
- 17 F. Faglioni, P. Lazzeretti, *Phys. Rev. A*, 2003, **67**, 032101.
- 18 R. Bast, P. Schwerdtfeger, *Phys. Rev. Lett.*, 2003, **91**, 023001.
- 19 D. Figgen, A. Koers, P. Schwerdtfeger, *Angew. Chem. Int. Ed.*, 2010, **49**, 2941.
- 20 F. Bock, F. Fischer, W. A. Schenk, *J. Am. Chem. Soc.*, 2006, **128**, 68.
- 21 J. H. Merrifield, C. E. Strouse, J. A. Gladysz, *Organometallics*, 1982, **1**, 1204.
- 22 W. E. Buhro, A. Wong, J. H. Merrifield, G.-Y. Lin, A. C. Constable, J. A. Gladysz, *Organometallics*, 1983, **2**, 1852.
- 23 P. R. Lassen, L. Guy, I. Karame, T. Roisnel, N. Vanthuyne, C. Roussel, X. Cao, R. Lombardi, J. Crassous, T. B. Freedman, L. A. Nafie, *Inorg. Chem.*, 2006, **45**, 10230.
- 24 F. De Montigny, L. Guy, G. Pilet, N. Vanthuyne, C. Roussel, R. Lombardi, T. B. Freedman, L. A. Nafie, J. Crassous, *Chem. Comm.*, 2009, 4841.
- 25 F. De Montigny, R. Bast, A. Severo Pereira Gomes, G. Pilet, N. Vanthuyne, C. Roussel, L. Guy, P. Schwerdtfeger, T. Saue, J. Crassous, *Phys. Chem. Chem. Phys.* 2010, **12**, 8792.
- 26 J. W. Faller, A. R. Lavoie, *Organometallics*, 2000, **19**, 3957.
- 27 W. K. Rybak, A. Skarzynska, T. Glowiak, *Angew. Chem. Int. Ed.*, 2003, **42**, 1725.
- 28 E. Tazacs, A. Escande, N. Vanthuyne, C. Roussel, C. Le-scop, E. Guinard, C. Latouche, A. Boucekkine, J. Crassous, R. Réau, M. Hissler, *Chem. Comm.*, 2012, **48**, 6705.
- 29 K. R. Jain, W. A. Herrmann, F. E. Kuhn, *Coord. Chem. Rev.*, 2008, **252**, 556.

- 30 G. S. Owen, J. Arias, M. M. Abu-Omar, *Catalysis Today*, 2000, **55**, 317.
- 31 R. L. Harding, T. D. H. Bugg, *Tetrahedron Lett.*, 2000, **41**, 2729.
- 32 B. M. Fox, J. A. Vroman, P. E. Fanwick, M. Cushman, *J. Med. Chem.*, 2001, **44**, 3915.
- 33 J. Dixon, J. H. Espenson, *Inorg. Chem.*, 2002, **41**, 4727.
- 34 J. H. Espenson, X. Shan, Y. Wang, R. Huang, D. W. Lahti, J. Dixon, G. Lente, A. Ellern, I. A. Guzei, *Inorg. Chem.*, 2002, **41**, 2583.
- 35 T. B. Freedman, X. Cao, R. K. Dukor, L. A. Nafie, *Chirality*, 2003, **15**, 743.
- 36 P. J. Stephens, F. J. Devlin, *Chirality*, 2000, **12**, 172.
- 37 P. L. Polavarapu, J. He, *Anal. Chem.*, 2004, **76**, 61A.
- 38 A. -C. Chamayou, S. Luedeke, V. Brecht, T. B. Freedman, L. A. Nafie, C. Janiak, *Inorg. Chem.*, 2011, **50**, 11363.
- 39 F. Weigend, R. Ahlrichs, *Phys. Chem. Chem. Phys.*, 2005, **7**, 3297.
- 40 R. G. Pearson, *J. Am. Chem. Soc.*, 1963, **85**, 3533.
- 41 Gaussian 09, Revision A.1, M. J. Frisch, G. W. Trucks, H. B. Schlegel, G. E. Scuseria, M. A. Robb, J. R. Cheeseman, G. Scalmani, V. Barone, B. Mennucci, G. A. Petersson, H. Nakatsuji, M. Caricato, X. Li, H. P. Hratchian, A. F. Izmaylov, J. Bloino, G. Zheng, J. L. Sonnenberg, M. Hada, M. Ehara, K. Toyota, R. Fukuda, J. Hasegawa, M. Ishida, T. Nakajima, Y. Honda, O. Kitao, H. Nakai, T. Vreven, J. A. Montgomery, Jr., J. E. Peralta, F. Ogliaro, M. Bearpark, J. J. Heyd, E. Brothers, K. N. Kudin, V. N. Staroverov, R. Kobayashi, J. Normand, K. Raghavachari, A. Rendell, J. C. Burant, S. S. Iyengar, J. Tomasi, M. Cossi, N. Rega, J. M. Millam, M. Klene, J. E. Knox, J. B. Cross, V. Bakken, C. Adamo, J. Jaramillo, R. Gomperts, R. E. Stratmann, O. Yazyev, A. J. Austin, R. Cammi, C. Pomelli, J. W. Ochterski, R. L. Martin, K. Morokuma, V. G. Zakrzewski, G. A. Voth, P. Salvador, J. J. Dannenberg, S. Dapprich, A. D. Daniels, Ö Farkas, J. B. Foresman, J. V. Ortiz, J. Cioslowski, and D. J. Fox, Gaussian, Inc., Wallingford CT, 2009.
- 42 E. B. Wilson, J. C. Decius and P. C. Cross, *Molecular Vibrations: The Theory of Infrared and Raman Vibrational Spectra*, Dover Publications, Inc., New York, 1995.
- 43 P. J. Stephens, F. J. Devlin, C. F. Chabalowski and M. J. Frisch, *J. Phys. Chem.*, 1994, **98**, 11623.
- 44 A. D. Becke, *J. Chem. Phys.*, 1993, **98**, 5648.
- 45 S. J. Vosko, L. Wilk, M. Nusair, *Can. J. Phys.*, 1980, **58**, 1200.
- 46 J. P. Perdew, K. Burke, M. Ernzerhof, *Phys. Rev. Lett.*, 1996, **77**, 3865.
- 47 D. Andrae, U. Haeussermann, M. Dolg, H. Stoll, H. Preuss, *Theor. Chim. Acta*, 1990, **77**, 123.
- 48 M. J. Frisch, J. A. Pople, J. S. Binkley, *J. Chem. Phys.* 1984, **80**, 3265; M. M. Francel, W. J. Petro, W. J. Hehre, J. S. Binkley, M. S. Gordon, D. J. DeFrees and J. A. Pople, *J. Chem. Phys.* 1982, **77**, 3654.
- 49 DIRAC, a relativistic ab initio electronic structure program, Release DIRAC12 (2012), written by H. J. Aa. Jensen, R. Bast, T. Saue, and L. Visscher, with contributions from V. Bakken, K. G. Dyall, S. Du-billard, U. Ekström, E. Eliav, T. Enevoldsen, T. Fleig, O. Fossgaard, A. S. P. Gomes, T. Helgaker, J. K. Lærdahl, Y. S. Lee, J. Henriksson, M. Iliaš, Ch. R. Jacob, S. Knecht, S. Komorovský, O. Kullie, C. V. Larsen, H. S. Nataraj, P. Norman, G. Olejniczak, J. Olsen, Y. C. Park, J. K. Pedersen, M. Pernpointner, K. Ruud, P. Salek, B. Schim-melpennig, J. Sikkema, A. J. Thorvaldsen, J. Thyssen, J. van Stralen, S. Villaume, O. Visser, T. Winther, and S. Yamamoto (see <http://www.diracprogram.org>).
- 50 B. Numerov, *Publ. Obs. Central Astrophys. Russ.*, 1933, **2**, 188.
- 51 J. W. Cooley, *Math. Comput.*, 1961, **15**, 363.
- 52 L. Visscher, K. G. Dyall, *At. Data Nucl. Data Tables*, 1997, **67**, 207.
- 53 T. H. Dunning Jr., *J. Chem. Phys.*, 1989, **90**, 1007; D. E. Woon, T. H. Dunning Jr., *J. Chem. Phys.*, 1993, **98**, 1358.
- 54 L. Visscher, T. Saue, *J. Chem. Phys.*, 2000, **113**, 3996.
- 55 L. Visscher, *Theor. Chem. Acc.*, 1997, **89**, 68.